JOURNAL OF Materials CHEMISTRY

Crystalline perfection of 2-amino-5-nitropyridinium dihydrogenphosphate–arsenate hybrid crystals for non-linear optical properties

Julien Zaccaro,[a] José Baruchel[b] and Alain Ibanez*[a]

[a]*Laboratoire de Cristallographie, C.N.R.S., associé à l'Université J. Fourier et à l'Institut National Polytechnique de Grenoble, BP 166, F-38042, Grenoble Cedex 09, France*
[b]*European Synchrotron Radiation Facility, BP 220, F-38043 Grenoble Cedex, France*

Received 15th October 1998, Accepted 13th November 1998

We report on the optimisation of the crystal growth conditions of two hybrid organic–inorganic materials for non-linear optical applications. Joint studies of experimental growth conditions, crystal quality and optical transmission have shown that extended defects observed by X-ray diffraction topography in the first generation of the 2-amino-5-nitropyridinium dihydrogenphosphate and arsenate phases are directly linked to the presence of organic impurities. By enhancing the purity of the starting materials and the stability of the growth solutions we have achieved a high crystalline quality and an extreme transparency.

In the last four decades, the extended field of non-linear optical (NLO) applications (frequency conversion, optical parametric amplification, oscillation, *etc.*) has stimulated the search for highly non-linear materials. Inorganic crystals generally exhibit a wide transparency range and high mechanical, thermal and chemical stability. In addition, their crystal growth is rather well controlled but their quadratic NLO efficiencies remain limited compared to those of organic molecular crystals which can be two orders of magnitude higher.[1,2] This is due to highly polarizable molecules involving π-electrons. Unfortunately, due to low thermal and mechanical resistance, the use of organic molecular crystals are currently limited in industrial applications. Indeed, their crystal packing is only insured by weak intermolecular bonds (van der Waals or long hydrogen bonds) leading to critical growing, slicing and polishing of large crystals. In order to overcome these basic drawbacks and to take advantage of the unique NLO properties of organics and their structural flexibility through chemical synthesis, a strategy aimed at the production of very cohesive non-centrosymmetric packing of chromophores has recently been developed. Organic molecules with large non-linear susceptibilities are anchored onto inorganic or semi-organic matrices through short H-bonds in order to form polar organic–inorganic structures. Using the charge transfer molecule of 2-amino-5-nitropyridine (2A5NP), a series of deliberately engineered non-centrosymmetric structures built-up from herringbone motifs of chromophores has been synthesised. For instance, 2-amino-5-nitropyridinium dihydrogenphosphate[3] (2A5NPDP), 2-amino-5-nitropyridinium dihydrogenarsenate[4] (2A5NPDAs), 2-amino-5-nitropyridinium L-tartrate[5] (2A5NPLT), and 2-amino-5-nitropyridinium chloride[6] (2A5NPCl). These hybrid materials tend to combine the advantages of both organic and inorganic crystals. The first quadratic NLO characterisations to be done on 2A5NPDP[7,8] and 2A5NPDAs[9] showed that these organic–inorganic salts exhibit nonlinear coefficients as high as those of the best inorganic crystals used in NLO devices (KTP, BBO). On the other hand, higher coefficients are expected for the 2A5NPCl[10] and 2A5NPLT phases.[5b] Moreover, the mechanical, thermal and chemical properties of all these hybrid salts are significantly better than those of the corresponding organic molecular crystals. Thus, their crystal growth leads to large crystals (several cm^3) of bulk morphology and crystal plates can be easily sliced and polished for optical characterisations. These materials have a rather extended transparency window in the visible and near IR regions (0.41–1.6 μm).[7] Nevertheless, for NLO devices, these crystals must be extremely transparent because even a small amount of absorption of the laser pump can introduce an unacceptable beam distortion from thermal lensing. In practice the major factor limiting transparency is the absorption due to impurities or residual scattering of the laser beam by defects such as solvent inclusions, bundles of dislocations, domain boundaries or misoriented sectors. This partial absorption or scattering of the incident and converted laser beams reduces the NLO efficiency of the crystal, particularly its optical damage threshold (thermal effect). Thus, the required extreme transparency is achieved through a high purity and an important defect reduction in the crystals.

The first 2A5NPDP and 2A5NPDAs crystals grown were of a rather good crystal quality.[11] In this article we present, the necessary enhancement in purity and crystal quality based on joint studies of the experimental growth conditions, X-ray diffraction topography and optical transmission.

Experimental

Crystal growth in solution

2A5NP is a weak Brönsted base which can be promoted in strong acidic aqueous solutions ($pH < 2$) leading to its dissolution and to the formation of salts with the conjugate bases of the acids involved. Thus, the 2A5NPDP and 2A5NPDAs salts are obtained by dissolving the 2A5NP molecule in a H_3XO_4 ($X = P$, As) acid solution at 60 °C with a molar ratio of 1 : 2 : 8 for 2A5NP, H_3XO_4 and H_2O respectively. These organic–inorganic salts crystallise at room temperature as white microcrystalline powders by addition of acetone. The synthesis yields are close to 100%.

We carried out the crystal growth of these organic–inorganic salts in solution. The solvent initially used was an aqueous solution of the acid corresponding to the salt (H_3PO_4 for 2A5NPDP and H_3AsO_4 for 2A5NPDAs). Its concentration is chosen between 2 and 4 M in order to provide good solubility and solubility-temperature gradient, and to fulfil the condition $pH < 2$. Indeed, under these low pH values the 2A5NP molecule can gain a proton and the organic cation 2-amino-5-nitropyridinium ($2A5NP^+$) thus obtained can be associated with the conjugate base of the acid to give the hybrid salt. Their crystal growth is made by the standard temperature reduction (TR) method close to room temperature

$(30 < T/°C < 50)$. In order to obtain high quality crystals, the temperature decrease is limited to about 0.15 °C day^{-1}. This requires a high temperature precision (±0.002 °C)[12] to prevent a rapid and uncontrolled burst of growth leading to solvent inclusions or imperfections in the resulting crystals.

In addition, we developed two thermal gradient techniques based on liquid phase transport in horizontal (HTG) or vertical configurations (VTG).[13] The solute transport is driven by a temperature gradient between the dissolution zone (higher temperature) which contains the nutrient and the growth zone where seeds are placed. A good control of the growth mechanisms is achieved with limited thermal gradients ($\Delta T = 2$–4 °C) and a temperature stability of about ±0.01 °C. VTG is the most efficient method because the crystals seeds are rotated in the growth solution (forced convection) as in the TR method. This improves the homogeneity of the crystal/solution interface and stabilises the growth mechanisms thus avoiding solvent inclusion and veiling in the crystals.

Using the TR, HTG and VTG methods, we have obtained large (several cm^3) and optically clear crystals of 2A5NPDP and 2A5NPDAs salts. The optimisation of the growth conditions was achieved through the characterisation of the quality of the resulting crystals by X-ray diffraction topography.

X-Ray diffraction topography

With the third generation synchrotron sources, X-ray beams of very high quality have become available: high flux, extremely reduced divergence, spatial and spectral homogeneity over a large cross section. They allow the investigation of thick, absorbing materials with short exposure times and very high resolution of the recorded images. The topographs and rocking curves presented here were recorded at the ESRF at ID19 beamline using two different configurations.

The first method, so-called section topography, corresponds to a Laüe transmission geometry using a white beam (6–80 keV). The lower part of the photon energy spectrum ($E < 6$ keV) was absorbed (Al 6 mm thick) to avoid a heat load on the samples which might modify the image contrast or even damage the crystals. The X-ray beam is vertically limited by narrow slits (about 20 μm in our case) and the topographs recorded on photographic films (perpendicular to the beam) are diffracted images of virtual slices of the sample. Several reflections are recorded at once (Laüe diagram), and only a small part of the crystal is illuminated. Thus, the defect images are more easily distinguished than in typical transmission projection topography.

On the other hand, highly distorted and extended crystal regions can appear on the diffracted images through white beam wavelengths which satisfy the diffraction conditions and the corresponding large contrasts can hide the image of other defects on the topographs. For this reason, we also used monochromatic radiation. In this configuration, the beam is not limited in size ($H \times V = 20 \times 10$ mm) but is monochromatized (0.62 Å) by a double-crystal [Si(111)] monochromator. The sample is oriented in order to select one reflection, the 200 in our case, which is collected either on a photographic film (monochromatic topography) or on a scintillator counter for rocking curve measurements. In the latter case, the beam and the detector are fixed and the sample is rotated in the ω circle (ω scan).

Optical transmission spectrum

As previously shown,[7,14] the cutoff wavelength near the UV region of the 2A5NPDP and 2A5NPDAs crystals is due to an electronic transition of the organic chromophore. UV–VIS transmission spectra have been used to characterise the crystal quality through the transparency of the grown crystals and to evidence their organic impurities. The crystal cuts involved in this study are (100) cleaved plates which are perpendicular to the X dielectric axis. The transmission spectra were registered with a Perkin-Elmer λ9 spectrometer and the incident beam was successively polarized along the Y and Z dielectric axis for each sample.

Results and discussion

The crystal growth of the 2A5NPDP phase was first undertaken with the TR method. The starting hybrid salt was synthesised from commercial 2A5NP powder and purified by successive recrystallisations in acetone. H_3PO_4 (2–4 M, pH = 1–1.5) acidic solutions were used as solvents and the resulting crystals were optically clear but lightly brown coloured [Fig. 1(a)]. The first X-ray topographs recorded on these samples with a typical Lang Chamber displayed elongated defects (ED) oriented along the [001] direction[11] (about 100 μm along the ***c***-axis—or even more, up to millimetres—and 10 μm along the ***b***-axis). To complete this defect characterisation, we then used synchrotron X-ray topography. Fig. 2(a) and 2(b) are section topographs carried out in the ***ab*** and ***ac*** planes respectively on a similar 2A5NPDP crystal. The white lines, inclined along the diffraction direction, appearing on these topographs are an artefact arising from a dust on the 20 μm slits (phase contrast). As previously observed with the Lang method,[11] this crystal exhibits a large amount of ED with a typical black contrast and sharp boundaries. This specific contrast and the fact that white beam topographs are not sensitive to changes of interreticular spacings clearly show that ED are associated with misoriented regions. In addition, we can see on Fig. 2(a) that ED are more extended along the ***b*** axis (around 10 μm) than along the ***a*** axis (1–2 μm). Fig. 2(b) confirms that ED are preferentially elongated along the ***c*** axis and that they propagate along this orientation through all the growth. This defect propagation is specific to ED since dislocations (D) propagate generally almost perpendicularly to the natural growth faces. This particular point can be clearly observed in Fig. 3 displaying a monochromatic topograph of the whole dome of the same crystal. On the other hand, in spite of their large size, the ED cannot be observed by optical microscopy, even between the crossed polarisers and analyser. This indicates that the refractive index difference associated with these ED is very low ($\Delta n < 10^{-3}$). Thus, these defects do not contain any heavy element or organic molecule very different from 2A5NP. Moreover, these defects were not only found in 2A5NPDP and 2A5NPDAs crystals grown by TR, VTG and HTG methods but also by gel-growth techniques.[8] Thus, the formation of ED is independent of the growth method, salt transport (purely diffusive in the gel-growth technique and

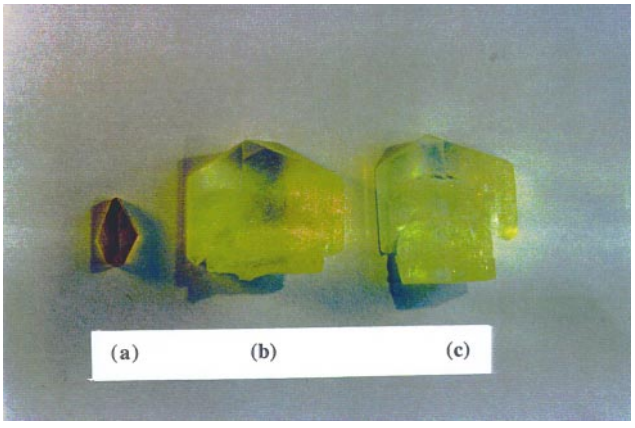

Fig. 1 Photographs of 2A5NPDP crystals of different purity grades, (a) grown from partially purified starting salt (only by recrystallisation) and pH 1–1.5 growth solutions, (b) from 2A5NP purified by successive sublimations and pH 1–1.5 growth solutions, (c) from 2A5NP purified by successive sublimations, pH 0.5 and deoxygenated growth solutions.

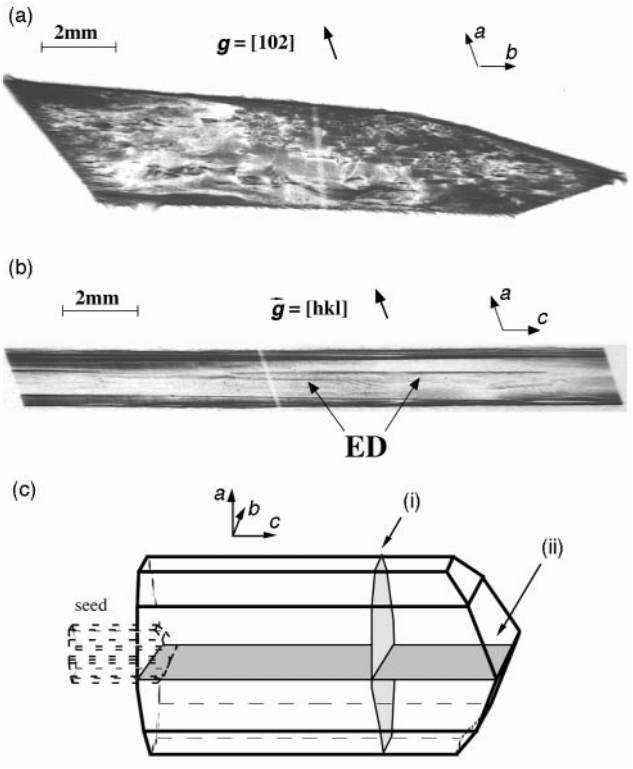

Fig. 2 Section topographs in ***ab*** (a) and ***ac*** (b) planes showing the ED morphology: tubular along the *c*-axis and wider along the *b*-axis than along the *a*-axis. These topographs were recorded as indicated on the schematic drawing (c).

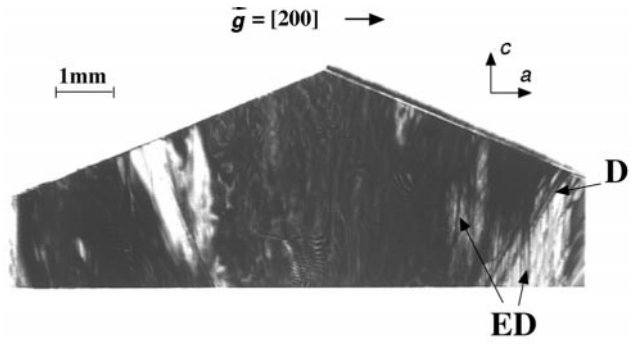

Fig. 3 Monochromatic topograph of the dome of the same 2A5NPDP crystal as in Fig. 2, showing the ED extension along ***c*** whereas dislocations (D) propagate almost perpendicularly to the growth faces.

forced convection in the TR and VTG methods) and solution homogeneity.

As no heavy element (other than P or As) has been found by X-ray fluorescence analysis in the 2A5NPDP and 2A5NPDAs crystals, in agreement with optical microscopy, we have suggested that ED would be due to the segregation of organic impurities. This would lead to local changes of impurity concentration inducing the formation of misoriented regions with respect to the crystal matrix. This hypothesis would explain the shape of these defects (elongated along the ***c*** axis and more extended along the ***b*** than the ***a*** axis) by an easier insertion of the organic impurities between the dense (100) mineral planes ($[H_2XO_4^-]_n$ with X = P or As). Indeed these (100) planes, connected between themselves by the weakest hydrogen bonds of the structure, correspond to the cleavage plane of these crystals (Fig. 4). In order to confirm this hypothesis and to avoid the formation of ED, we strove to identify and eliminate all the organic impurity sources.

First, we improved the purity of the starting materials by successive sublimations of the commercial 2A5NP (only 98%

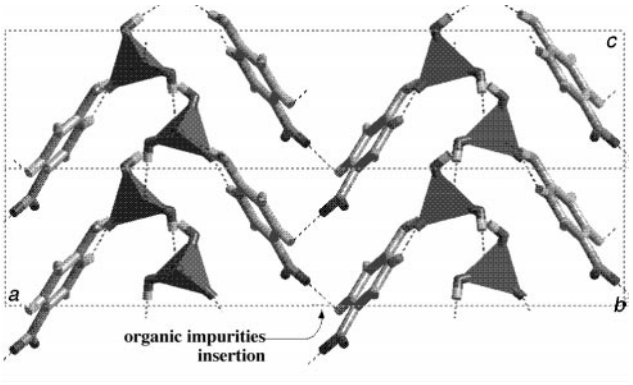

Fig. 4 Projection along ***b*** of the 2A5NPDP(As) structure (***c***-axis is vertical) showing the mineral planes built up from $[H_2XO_4]_n$ tetrahedra while the 2A5NP organic molecules are anchored to these planes by short H-bonds. The 2A5NP molecules are connected by the weakest H-bonds (C–H···O) of the structure corresponding to the (100) cleavage plane.

pure) and using high purity grade acids for the salt synthesis. The 2A5NPDP(As) phases were purified by recrystallisations in acetone. Then, a second set of crystal growths was undertaken under the same experimental conditions as before (see above). The enhancement of purity induced a significant decrease in the 2A5NPDP(As) crystal colouring, turning from light brown to yellow [Fig. 1(b)]. This is associated with an important reduction of the amount of ED as illustrated in Fig. 5 which shows a section topography recorded in the ***ab*** plane of a 2A5NPDP crystal. Moreover, the ED seems to induce important strains in the crystal leading to distorted regions appearing as black–white contrasts, which correspond, for the 221 reflection selected for this section topography, to the experimental absorption condition $\mu t \approx 2$.[15]

The remaining of some ED after these purification steps suggests that the starting materials are not the only source of organic impurities in solution. This explains the yellow coloration of these crystals which remains different to the intrinsic colour of the hybrid salts family based on the 2A5NP molecule (slightly green[12]). In addition, a colour evolution of the growth solution, from yellow to slightly brown, is always observed after several months. Since the initial organic impurities are removed by successive sublimation, the 2A5NP molecule is now the only source of organic impurity. Thus, the yellow and brown crystal colouring must be due to the incorporation of this chromophore in the crystal structure under other forms than the $2A5NP^+$ cation.

In solution, the $2A5NP^+$ can be destabilised in two forms. The first one is the 2A5NP unprotonated molecule, its amount in solution can be directly connected to the pH value according to the simplified equilibrium:

$$C_5H_6O_2N_3^+ + H_2O \rightleftharpoons C_5H_5O_2N_3 + H_3O^+$$

Thus, the concentration of unprotonated 2A5NP molecule in solution increases with pH value. As previously shown,[7] the protonation in solution of 2A5NP induces a blue shift of its λ-cutoff wavelength toward the UV region of about 40 nm,

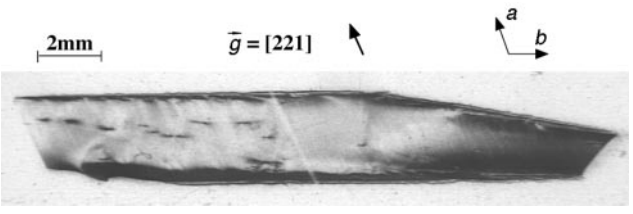

Fig. 5 Section topograph in the ***ab*** plane showing the important reduction of ED upon total elimination of the organic impurity arising from the commercial 2A5NP.

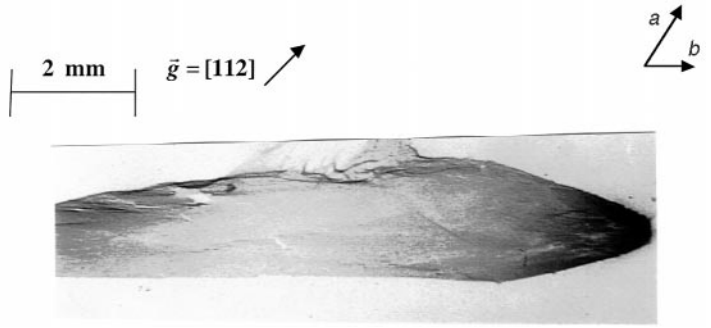

Fig. 6 Section topograph in the ***ab*** plane of a 2A5NPDAs crystal showing complete absence of ED: this diffracted image displays homogeneous intensity.

decreasing its colouration from yellow to slightly green. Thus, we can assign the yellow colour of the crystals to the incorporation of unprotoned 2A5NP molecules during the growth. To reduce this 2A5NP concentration in solution it is necessary to significantly decrease the pH value. Unfortunately, it is not possible to choose as solvents orthophosphoric or arsenic acids at concentrations higher than 4 M because the solubility and solubility–temperature gradient become too important and not at all suited to a good control of the supersaturation applied (*ca*. 0.01) in the crystal growths. In order to achieve lower pH values, we selected acetic acid as a solvent because it possesses several advantages. Its acidity is too weak to form a salt (acetate) with the 2A5NP molecule but at high concentrations (*ca*. 16.5 M) we can reach very low pH values (pH *ca*. 0.5) while the solubility and solubility–temperature gradient remain in a useful range.[11]

On the other hand, previous work, made on other organic molecules, has proved that the amine function can be oxidized to a nitro group and that this oxidation is prevented at low pH values ($pH \approx 0$). In our case, the amine oxidation takes place certainly on the unprotonated 2A5NP chromophore leading to the formation of the 2,5-dinitropyridine (2,5-DNP) molecule.[16,17] This reaction is associated with an important change in molecular electronic transitions because an electron-donor group (NH_2) is replaced by an electron-acceptor group (NO_2). Thus, the charge transfer of the molecule is strongly reduced (as its non-linear susceptibility), and the corresponding electronic transition is shifted toward higher wavelengths. In addition, this oxidation seems to be photoassisted since growth solutions turn brown in a few days when they are directly exposed to sunlight.

The low pH values reached using acetic acid (16.5 M) as a solvent allow us to stabilise the amine function of 2A5NP in solution. Nevertheless, in order to eliminate any residual oxidation, the growth solutions are systematically deoxygenated by a circulation of nitrogen gas and covered with an oil film to avoid oxygen reabsorption. Under these experimental conditions we obtained, with the TR method, optically clear crystals with a very slight green coloration [Fig. 1(c)] corresponding to the intrinsic colour of these hybrid salts. Moreover, no colour change of the growth solutions was observed, even after several months. In Fig. 6, we show a section topography recorded in the ***ab*** plane of an as-grown 2A5NPDAs crystal. The direct comparison of Fig. 2, 5 and 6 illustrates the significant enhancement of crystalline quality. The ED removal by elimination of all the sources of organic impurities leads to weak image contrast of X-ray diffraction topography (Fig. 6). The asterism appearing on the upper part of the image (weak contrasts) is linked to extrinsic strains[18] produced on the crystal edge by an unwitting handling. A small contrast allows the observation of two slightly misoriented regions. The little points observed at the bottom of the image could be isolated dislocations intersecting the section plane while the central zone appears free of defects.

On the other hand, in order to globally quantify the improvement of crystal quality with purity, we measured X-ray diffraction rocking curves. In Fig. 7 we compare the rocking curve of a 2A5NPDP crystal of first generation containing a high amount of ED (see the corresponding section topograph on Fig. 2) with a last generation one, ED free. The ED vanishing induces a sharpening of the rocking-curve, indeed the FWHM decreases from about 1.7′ to 25″ while the calculated diffraction width[15] for this 200 reflection (Darwin width) is $\varepsilon = 0.9''$. For the first sample, it is difficult to determine the FWHM since the rocking curve exhibits an asymmetric intensity distribution (Fig. 7).

In order to confirm the ED origin and to specify their impact on the optical properties of 2A5NPDP(As) crystals we registered the optical transmission spectra of three 2A5NPDP samples of different purity grade (Fig. 8). Sample 1 was a first generation crystal purified only by a salt recrystallisation which leads to a high ED content (Fig. 2), sample 2 was grown from high purity salt (2A5NP double sublimation and salt recrystallisation) but using a pH solvent value too high (1–1.5) to completely stabilise the $2A5NP^+$ in solution (low ED content, Fig. 5) and sample 3 was a last generation crystal (high purity starting materials, solvent $pH \approx 0$, ED free, Fig. 6). One can observe on the transmission spectrum of sample 1 that the transmission maximum is limited to 65%. This optical limiting cannot be explained only by reflection losses (around 12% in this case). Moreover, two additional absorption bands, A and B, appear clearly in the transparency window, A is approximately centred at 0.46 μm and B at 0.58 μm. From comparison with the spectrum of sample 2, we can conclude that the B absorption band is due to a 2A5NP organic impurity which disappears with sublimation. The removal of this type of impurity induces also an enhancement of the transmission to

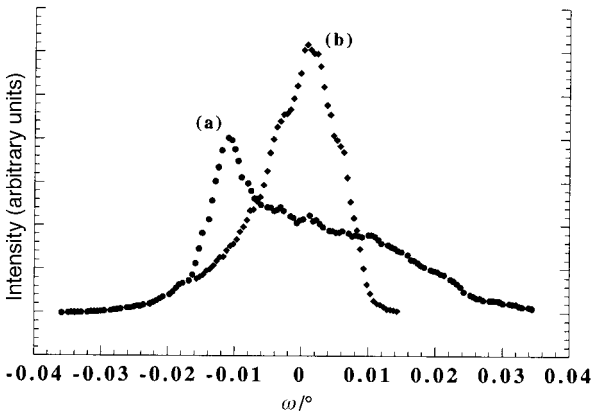

Fig. 7 X-Ray diffraction rocking curves of different purity grade crystals. (a) 2A5NPDP crystal containing a high ED content and corresponding to the topograph shown in Fig. 2, (b) 2A5NPDP crystal free of ED (see topograph in Fig. 6).

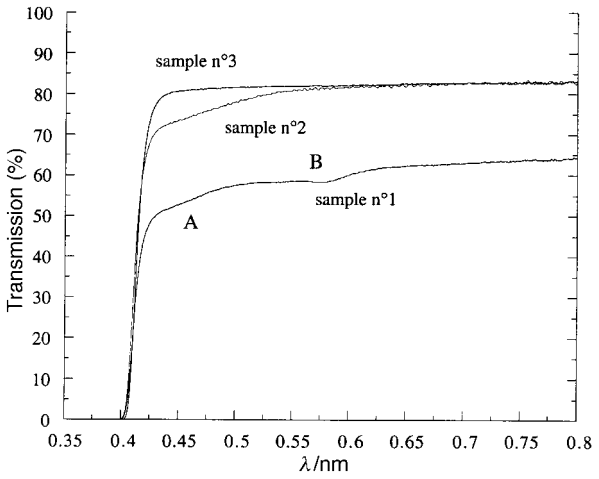

Fig. 8 Transmission spectra of 2A5NPDP *X*-cuts of different purity grades recorded with polarised light along ***b*** (*Y*=dielectric axis). Sample 1 corresponds to a first generation crystal, sample 2 is a crystal of low ED content and sample 3 is ED free.

about 83%. The limited transmission of sample 1 can be explained by this impurity absorption in the visible region and by the light diffusion of the ED whose number is significantly reduced in sample 2. On the other hand, the A absorption band at 0.46 μm is still present for sample 2 but disappears for sample 3 with the $2A5NP^+$ stabilisation in the growth solution. Hence, the A band is certainly associated with the $2A5NP^+$ destabilised forms (unprotonated 2A5NP and/or oxidized, 2,5DNP), its wavelength position being in good agreement with the observed blue shift of the λ-cutoff between the 2A5NP molecule and its protonated form. The total elimination of these additional absorption bands is an important elaboration step in the aim to carry out NLO devices with this family of hybrid materials.

Conclusions

We have specified that the elongated defects (ED) observed by X-ray diffraction topography in the first generation crystal of the 2A5NPDP(As) hybrid phases are directly connected to the presence of organic impurities and that their orientation in the crystals is different from the typical ones of dislocations. Indeed, ED are not extended perpendicularly to the growing faces but along the ***c*** axis and are not refracted when they cross growth sector boundaries. The formation mechanism of these defects remains an open question. They may be generated either by a segregation of the organic impurities at the growth front or by their diffusion and aggregation behind this front in the solid state. Since ED cannot be eliminated through crystal growth like dislocations, to remove them it was necessary to eliminate all sources of organic impurities. The two possible impurity sources we identified come from the commercial 2A5NP powder and from the $2A5NP^+$ destabilisation in solution under the unprotonated or the oxidised forms. The first impurity type is removed by successive sublimations of the 2A5NP starting material. The stabilisation of the $2A5NP^+$ cations in the growth solutions is achieved by using low pH solvents ($pH \approx 0.5$) and by deoxygenating these solutions with a nitrogen gas circulation. The optimisation of the growth experimental conditions allow us to significantly improve the crystalline quality and purity of the 2A5NPDP(As) crystals leading to a significant enhancement of their transparency window. This opens the way to the fabrication of NLO devices with this new hybrid crystal family.

Acknowledgements

The authors would like to thank R. Masse for fruitful discussions, D. Block and M. Chamel for optical characterisations and J. Haërtwig for his help in rocking curve acquisitions.

References

1 J. Zyss, J. F. Nicoud and M. Coquillay, *J. Chem. Phys.*, 1984, **81**, 4160.
2 I. Ledoux, J. Badan, J. Zyss, A. Migus, D. Hulin, J. Etchepare, G. Grillon and A. Antonetti, *J. Opt. Soc. Am. B*, 1987, **4**, 987.
3 R. Masse and J. Zyss, *Mol. Eng.*, 1991, **1**, 141.
4 J. Pécaut, Y. Lefur and R. Masse, *Acta Crystallogr., Sect. B*, 1993, **49**, 535.
5 (*a*) J. Zyss, R. Masse, M. Bagieu-Beucher and J. P. Lévy, *Adv. Mater.*, 1993, **5**, 120; (*b*) O. Watanabe, T. Noritake, Y. Hirose, A. Okada and T. Kurauchi, *J. Mater. Chem.*, 1993, **3**, 1053.
6 J. Pécaut, J. P. Levy and R. Masse, *J. Mater. Chem.*, 1993, **3**, 999.
7 Z. Kotler, R. Hierle, D. Josse, J. Zyss and R. Masse, *J. Opt. Soc. Am. B*, 1992, **9**, 534.
8 N. Horiuchi, F. Lefaucheux, M. C. Robert, D. Josse and J. Zyss, *J. Cryst. Growth*, 1995, **147**, 361.
9 J. P. Feve, B. Boulanger, I. Rousseau, G. Marnier, J. Zaccaro and A. Ibanez, *IEEE Quantum Elect.*, in press.
10 N. Horiuchi, F. Lefaucheux, A. Ibanez, D. Josse and J. Zyss, *J. Opt. Mater.*, in press.
11 J. Zaccaro, B. Capelle and A. Ibanez, *J. Crystal Growth*, 1997, **180**, 229.
12 A. Ibanez, J. P. Levy, C. Mouget and E. Prieur, *J. Solid State Chem.*, 1997, **129**, 22.
13 J. Zaccaro, M. Bagieu-Beucher, J. Espeso and A. Ibanez, *J. Crystal Growth*, 1998, **186**, 224.
14 J. Zaccaro, D. Block, M. Chamel and A. Ibanez, *J. Opt. Soc. Am. B.*, submitted.
15 *Applications of X-ray Topographic Methods to Materials Science*, ed. W. Weissman, F. Balibar and J. F. Petroff, Plenum, New York, 1984.
16 E. C. Taylor, C. P. Tseng and J. B. Rampal, *J. Org. Chem.*, 1982, **47**, 552.
17 O. Rakitin, O. Vlasova and L. Khmel'nitskii, *Chem. Heterocycl. Compd.*, 1990, **26**, 1281.
18 A. Guinier, *Theorie et Technique de la Radiocristallographie*, Dunod, Paris, 1956.

Paper 8/08016J